AGU ADVANCING EARTH AND SPACE SCIENCE

Geophysical Research Letters

RESEARCH LETTER
10.1029/2021GL095464

Tropospheric Role in the Predictability of the Surface Impact of the 2018 Sudden Stratospheric Warming Event

Juan J. González-Alemán[1,2], Christian M. Grams[3], Blanca Ayarzagüena[1], Pablo Zurita-Gotor[1,2], Daniela I. V. Domeisen[4,5], Iñigo Gómara[1,2], Belén Rodríguez-Fonseca[1,2], and Frédéric Vitart[6]

[1]Departamento de Física de la Tierra y Astrofísica, Universidad Complutense de Madrid, Madrid, Spain, [2]Instituto de Geociencias (IGEO), UCM-CSIC, Madrid, Spain, [3]Department Troposphere Research, Institute of Meteorology and Climate Research (IMK-TRO), Karlsruhe Institute of Technology (KIT), Karlsruhe, Germany, [4]ETH Zurich, Institute for Atmospheric and Climate Science, Zurich, Switzerland, [5]University of Lausanne, Lausanne, Switzerland, [6]European Centre for Medium-Range Weather Forecasts, Reading, UK

Key Points:

- The surface impact of the sudden stratospheric warming in 2018 was associated with a Greenland blocking in the troposphere
- Medium-range uncertainties in the prediction of the Greenland blocking were linked to two cyclogenesis events over the North Atlantic
- Individual synoptic events constitute "predictability barriers" for subsequent forecast lead times after sudden stratospheric warming events

Supporting Information:

Supporting Information may be found in the online version of this article.

Correspondence to:

J. J. González-Alemán,
juanjego@ucm.es

Citation:

González-Alemán, J. J., Grams, C. M., Ayarzagüena, B., Zurita-Gotor, P., Domeisen, D. I. V., Gómara, I., et al. (2022). Tropospheric role in the predictability of the surface impact of the 2018 sudden stratospheric warming event. *Geophysical Research Letters*, *49*, e2021GL095464. https://doi.org/10.1029/2021GL095464

Received 5 AUG 2021
Accepted 11 DEC 2021

Abstract Sudden stratospheric warmings (SSWs) can have a strong impact on the troposphere. Their fingerprint is often associated with the negative phase of the Northern Annular Mode (NAM) and the North Atlantic Oscillation (NAO), and extreme weather with high societal impact. However, the mechanisms behind this downward impact are not well understood. We investigate this surface impact through its associated predictability limits, by studying the 2018 SSW event. We search for predictability barriers that occurred after the onset of the SSW and before its surface impact. It is found that dynamical tropospheric events consisting of two cyclogenesis events were the main reasons for these predictability barriers in the prediction of negative NAM/NAO anomalies reaching the surface. This work corroborates that individual synoptic events might constitute predictability barriers during the downward impact of SSW events, and thereby sheds light on stratosphere-troposphere coupling.

Plain Language Summary Sudden stratospheric warmings (SSWs) can have a strong impact on near-surface weather. They have the potential to alter the atmospheric circulation and associated extreme events, thus affecting society. However, the way the stratosphere couples with surface weather is not fully understood. In this work, we investigate this relationship by analyzing the predictability of the surface impact of a stratospheric warming event that occurred in 2018, and which left widespread societal impacts over Europe due to a severe cold spell and extraordinary rainy and windy conditions. We find that the impact of this SSW event on the surface was regulated by two low-pressure systems that developed over the North Atlantic. Even though the SSW event was well developed, alternative behavior of these systems could have led to drastically different weather conditions over Europe. Thus, this study highlights the role of the tropospheric circulation in the effectiveness of the stratospheric impact on surface weather.

1. Introduction

Predictability barriers are sudden changes in the numerical ensemble predictability of the atmospheric flow. At synoptic time scales, these jumps are associated with events that are crucial for the subsequent development of major circulation changes (Meehl et al., 2021; Sánchez et al., 2020). Predictability barriers occur because the forecast system has difficulty in simulating particular events and/or these events have low intrinsic predictability. As long as these events are not well simulated by the prediction system, the presence of predictability barriers compromises the forecasting accuracy of subsequent events. Thus, a better understanding and representation of the jump-related phenomena is highly necessary for improving the prediction of major flow changes.

As will be shown in this study, several predictability barriers can be identified in the forecasts of the ECMWF Ensemble Prediction System (ECMWF, 2020) in February 2018 before high-impact weather affected Europe. A severe cold spell was observed over large parts of northern Eurasia, from the end of February–March 2018, along with a period of extraordinary rainy and windy conditions in southwestern Europe. These events were associated with a rapid change of the tropospheric circulation from prevailing westerlies into a blocked state (Greenland Blocking) in the North Atlantic, which caused an abrupt shift of the North Atlantic Oscillation (NAO) toward its negative phase (hereafter NAO-) at the end of February 2018 (Ayarzagüena et al., 2018; Kautz et al., 2020). This sudden change in the circulation was preceded by high synoptic-scale activity, with a series of strong upstream extratropical cyclones that triggered large-scale Rossby wave-breaking events (Colucci, 1985; Gómara et al., 2014; Michel et al., 2012) over the North Atlantic from mid- to end of February. These cyclones transported warm and humid air from the subtropics toward high latitudes associated with their warm conveyor belts, which promoted the establishment of a blocking ridge (Binder et al., 2017; Grams et al., 2018; Maddison et al., 2019; Pfahl et al., 2015; Steinfeld et al., 2020).

At the same time, a sudden stratospheric warming (SSW) event took place on 12 February 2018. Evidence points toward a role of this SSW event in the shift toward the negative NAO phase (Ayarzagüena et al., 2018) and in providing extended-range tropospheric predictability (Kautz et al., 2020; Rao et al., 2020). SSWs are rapid breakdowns of the stratospheric polar vortex (Baldwin et al., 2021) that can have a strong impact on the troposphere, preceding shifts in the probability distributions of the Arctic Oscillation and NAO, and in the location and strength of the extratropical jet stream and storm tracks (Baldwin & Dunkerton, 1999, 2001). Thus, they may be used as predictors of changes in the tropospheric weather. During the last 20 years, a range of tropospheric extreme events with high societal impact have been linked to SSWs (Domeisen & Butler, 2020). However, the mechanisms behind the downward impact of SSWs, such as the role played by tropospheric synoptic-scale processes, are insufficiently understood (Baldwin et al., 2021; Domeisen et al., 2013; Rupp & Birner, 2021). Consequently, it is unclear why some SSWs have a strong impact on the troposphere, while the fingerprint of some others is almost negligible. Internal tropospheric variability has been suggested as an important factor in determining the downward response of SSW events (Chan & Plumb, 2009; Domeisen, Grams, & Papritz, 2020; Garfinkel et al., 2013).

This study investigates the synoptic tropospheric events following the 2018 SSW and preceding the abrupt shift into the NAO- state at the end of February 2018 which may have favored the emergence of the surface impact of the SSW. We aim to understand which individual synoptic events might have constituted major “predictability barriers" for subsequent forecast lead times and to shed light on stratosphere-troposphere coupling through a better understanding of the role of tropospheric dynamics.

2. Data and Methods

2.1. ECMWF Ensemble Prediction System

This study is based on ensemble predictions from the European Center for Medium-Range Weather Forecasts (ECMWF) Integrated Forecasting System (IFS, Cycle 41r2: ECMWF, 2020), which became operational in 2016. Operational analysis, control and 50 perturbed ensemble forecasts (EPS) are used to perform the analysis. Initializations cover the period 1–28 February 2018 with a medium-range forecast horizon (i.e., 15 days). The spectral resolution of the analysis is TCO1279/O1280 (~9 km) using 137 vertical levels and TCO639/O640 (~18 km) with 91 vertical levels for the ensemble forecast. ERA-Interim reanalysis data (Dee et al., 2011) are used as observational reference (1979–2018).

2.2. Atlantic-European Weather Regimes

To investigate the evolution of the large-scale circulation in the ensemble forecast we consider forecasts of Atlantic-European weather regimes (WRs). WRs are identified based on the extended year-round classification of Grams et al. (2018), using seven different regimes, which reflect the preferred flow patterns within the variability of the atmospheric circulation in the Atlantic–European region. These regimes are based on a k-means clustering in the phase space spanned by the leading seven empirical orthogonal functions (EOFs) of ten-day low-pass filtered 500 hPa normalized geopotential height anomalies in the Atlantic–European sector taken from ERA-Interim reanalysis for 1979–2015. The regime in each ensemble member and analysis is derived from the projection of the instantaneous unfiltered normalized 500 hPa geopotential height anomaly on the cluster mean.

A WR index (IWR) is calculated as the anomaly of the projection normalized by the standard deviation following Michel and Rivière (2011). The IWR is computed at each time step and for each regime. A member is attributed to an active WR at a given time step if the respective IWR is greater than 1.0 and greater than that of all other WRs. The seven regimes used are as follows: the Zonal regime (ZO) and its variant Atlantic Trough (AT); the related Scandinavian Trough (ScTr) and Atlantic Ridge (AR) regimes; European Blocking (EuBL) and Scandinavian Blocking (ScBL); and Greenland Blocking (GL), which corresponds to NAO-. For better comprehension of the results, the analysis is focused on GL, AR and EuBL, which includes the majority of the probability distribution within the period of study. For further information on regime characteristics see Beerli and Grams (2019).

2.3. Northern Annular Mode

The Northern Annular Mode (NAM) is defined as the first empirical orthogonal function (EOF) of the monthly mean geopotential height anomalies poleward of 20°N (Baldwin & Dunkerton, 2001). The EOF analysis is applied to ERA-Interim data at each pressure level separately (10, 50, 100, 200, 250, 300, 400, 500, 700, 850, 925 and 1,000 hPa) for the extended winters (December to March) of the period 1981–2010. The 6-hourly data of the IFS output is then regressed onto the spatial patterns of the NAM at each pressure level to compute the NAM index at the corresponding level for each ensemble member and for each time step of this forecast.

3. Identification and Analysis of Predictability Barriers

To identify discernible predictability barriers for the change toward NAO- conditions at the end of February and early March 2018, we investigate the probability of GL occurrence for different initialization times (Figure 1). The forecast evolution indicates two first major predictability barriers for the target temporal window (27 February–3 March), where there is an increase in likelihood of more than 25% (Figure 1b): (a) Forecasts prior to the initialization of 12 February 2018 show low probability (less than 25% of ensemble members) of GL. (b) From the initialization of 17 February 2018 onwards at least 50% of the ensemble members correctly indicate the occurrence of GL. The first jump occurs in association with the onset of the SSW. Between the two jumps there is also high variability in the GL probability, as reflected in probability ranging from ∼50% to ∼70%. The 00 UTC 17 February 2018 initialization is the last one before almost all ensemble members predicted the occurrence of GL. We first focus on this last poor initialization (00 UTC 17 February 2018) and the prediction of GL on 1 March, when the regime was well-established (Figure S1b of Supporting Information S1).

4. Tropospheric Dynamical Causes

The second jump in predictability is the most important one as it leads to the final overall increase of GL occurrence (Figure 1). To understand the physical causes, we construct composites based on the prevalent WRs at 288 hr of forecast (hereafter reference time) after the initialization time 00 UTC 17 February 2018, i.e., 00 UTC 1 March 2018. Each composite is produced by computing the mean for all the ensemble members belonging to each WR (at the reference time) for the corresponding forecast time. The statistical significance of the differences between two weather regimes' composites is computed through the p-value (≤ 0.05) of a two-sided Wilcoxon rank sum test (Wilks, 2006). At the reference time, 18 out of 51 ensemble members already simulate the development of GL, which is already well established in the analysis (see Figure S1 in Supporting Information S1).

Figure 2 shows the results from the composite analysis. The first noticeable region of errors starts to develop in the EuBL composite in the MSLP field at 60 forecast hours to the east of Newfoundland (Figure 2 top right). These errors in the MSLP field are not as prominent in the GL and AR composites (Figure 2 top central and left). They are mainly located to the north of a strong extratropical cyclone (C1), which developed by 19 February 2018 south of Newfoundland and moved eastward. These errors are dynamically associated with precipitation processes (Figures S2 and S3 in Supporting Information S1) occurring within the cyclonic region. These processes promote different behavior between composites in the manner C1 forms, evolves and triggers its associated Rossby wave breaking (RWB). The region of errors grows with time as the low-pressure system reaches its mature phase.

At 168 forecast hours, the geopotential field at 500 hPa in the EuBL composite (Figure 2, bottom right) also shows a region with large errors north and south of Iceland, associated with the previous ones (60 hr) in the MSLP field over the central North Atlantic (cf. temporal evolution of MSLP and Z500 forecast in Figures S4 and S5 of Supporting Information S1). The errors are again weaker for AR and, especially, GL (Figure 2 bottom central and left). In this case, errors are associated with RWB events associated with C1 and a subsequent secondary cyclone (C2), which emerges from C1 once it reaches the Azores to the northeast and moves northward. These RWB events can be seen in Figure 2 from Kautz et al. (2020). From a dynamical point of view, biases in RWB are associated with errors in the North-Atlantic eddy momentum flux (Figure S6 in Supporting Information S1) and in the position of the North-Atlantic jet, being GL the composite more similar to the analysis. Different C2

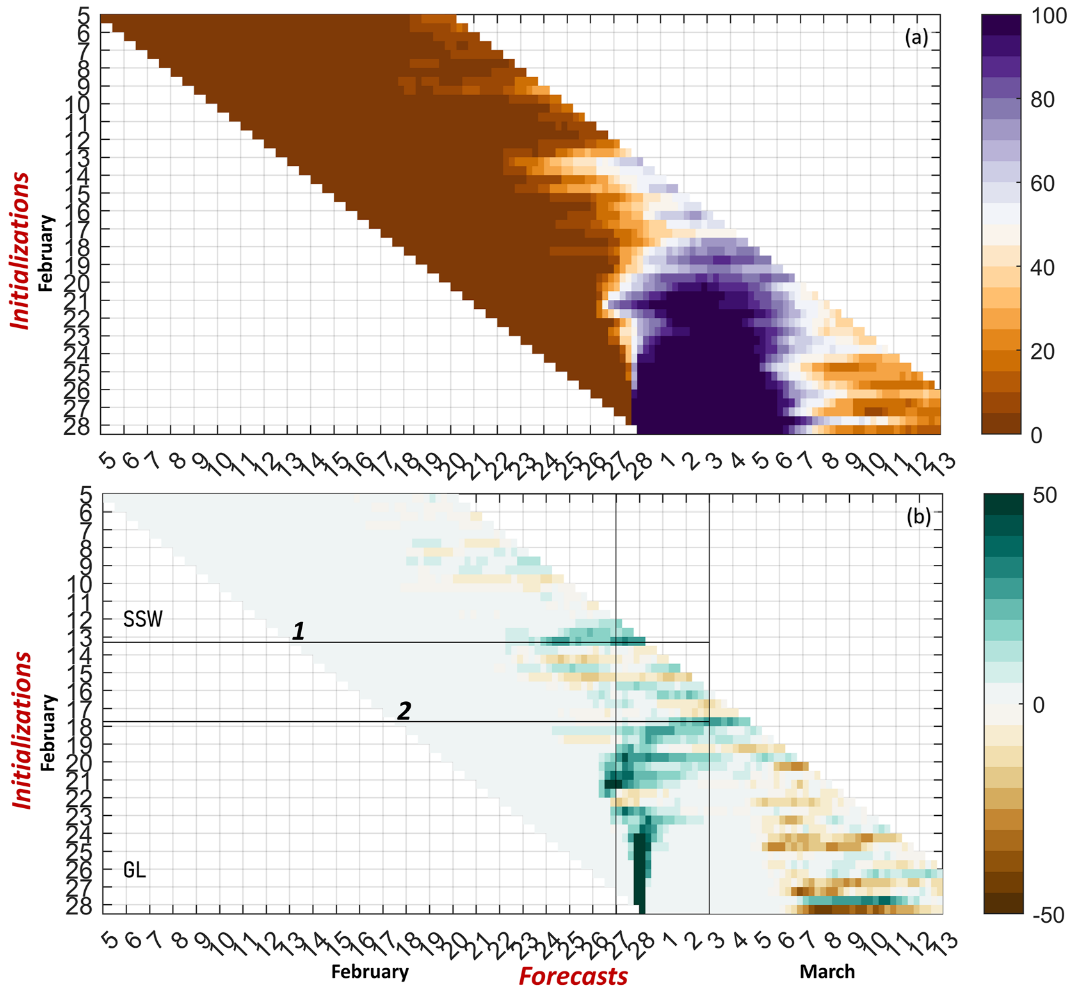

Figure 1. (a) Probability (%) of Greenland Blocking occurrence based on the initialization and forecast times from the European Center for Medium-Range Weather Forecasts Ensemble Prediction System. (b) Same as (a) but forecast changes as the difference in probability of the current to the previous initialization time. The observed onset of the sudden stratospheric warming and the Greenland Blocking is indicated with sudden stratospheric warming and GL, respectively. Predictability barriers studied in this study are indicated with numbers and horizontal lines. Vertical lines indicate the target temporal window.

behavior among WRs is dynamically related to cyclogenesis processes like warm and humid air advection from the subtropics promoted by C1 (Figure S7 in Supporting Information S1). This evolution of errors suggests, thus, an important contribution of C1 and its subsequent cascade of events for the development of GL. This idea is explored in more detail in the next section.

5. Consistency With Other Initializations

The conclusions from the previous analysis based on the 00 UTC 17 February 2018 initialization are consistent with previous and subsequent initializations. Figure 3 shows how the WRs probability changes with initialization time. We investigate the accumulated probabilities for two groups of WRs based on key characteristics in the circulation pattern over the Euro-Atlantic region: Blocked regimes (BR) are those WRs associated with a ridge anomaly over the north-northeastern Atlantic (AR, EuBL, ScBL, GL), whereas cyclonic regimes (CR) are those associated with a trough anomaly over the same region (AT, ScTr, ZO) or no regime.

Two noticeable changes can be detected associated with the previously identified predictability barriers (12 and 17 February). The first one occurs between the initializations on 11 February, 12 UTC and 13 February 2018 at 12 UTC. A noticeable shift between the prevalence of cyclonic versus blocked regimes occurs in the forecast

10.1029/2021GL095464

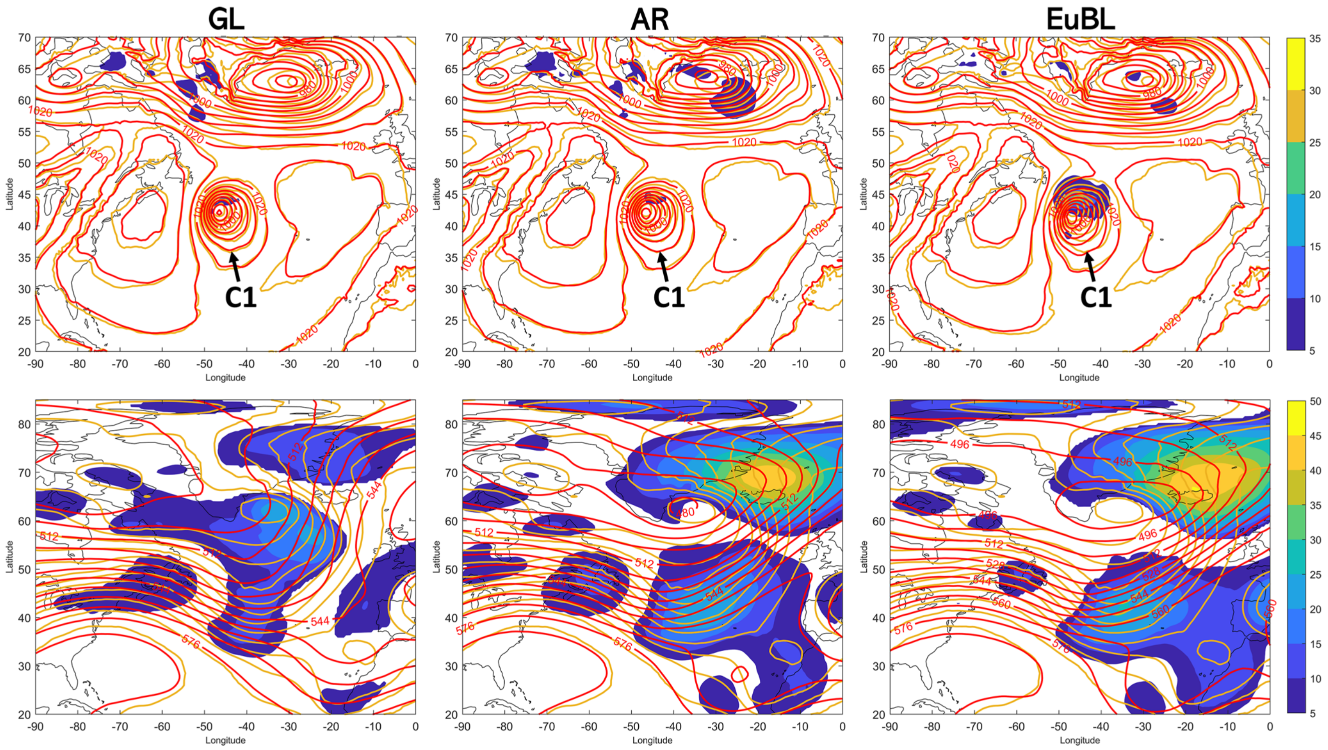

Figure 2. Upper row: Weather regime (WR) composite (red contours) and analysis (orange contours) for MSLP (hPa) at 60 hr of forecast from the 00 UTC 17 February 2018 initialization. Bottom row: Same as above but for 500-hPa geopotential height (damgp) at 168 hr. Errors (WR mean–analysis absolute values) are represented by shading. From left to right: composites for members attributed to the GL, AR and EuBL.

for 20 February 2018 (Figures 3a and 3b). This sudden jump in the probability of blocked regimes is associated with a better representation of C1 in the EPS; the prediction changes between those initializations from a robust anticyclone to a shallow low in the ensemble mean (Figures 3c and 3d).

The second jump occurs between the initializations on 17 February, 00 UTC and on 19 February 2018, 12 UTC, where a large increase in GL probability occurs in the forecast from 26 February onwards (Figures 3e and 3f). This sudden increase is associated with an improved simulation of C2 in the EPS; the low in the ensemble mean deepens and thereby aligns with the observed development (Figures 3g and 3h).

6. Potential Connections to the Stratosphere and the Ocean

To provide a broader perspective of the atmospheric dynamical processes at play during late February 2018, the stratosphere-troposphere evolution based on the 00 UTC 17 February 2018 initialization is represented in Figure 4. Strong observed NAM- values can be identified (Figure 4a) at 10 hPa around 100 hr from initialization, which can be associated with the SSW (Ayarzagüena et al., 2018). These negative anomalies propagate downward to the lower stratosphere (~100 hPa) over time. In addition, another region of NAM- values develops in the lower troposphere (~925 hPa) around 200 hr and becomes strongest after 300 hr, which is associated with the circulation change toward a blocked state. The downward propagation of NAM- values connects to the tropospheric NAM- when reaching the lower stratosphere around 300 hr. This will be referred to as NAM connection.

Only the subset of members predicting GL on 1 March exhibits the observed NAM connection (Figure 4b). This happens around 300 hr of lead time, just when tropospheric NAM- values are most robust. The EuBL subset does not simulate this NAM connection (Figure 4d). Instead, NAM + values appearing around 150 hr in the upper troposphere become much stronger than both in the analysis and GL, which interferes with the NAM connection. Therefore, all ensemble members include the stratospheric perturbation related to the SSW but some do not show the expected fingerprint in the troposphere. This suggests that properly simulating cyclones C1 and C2,

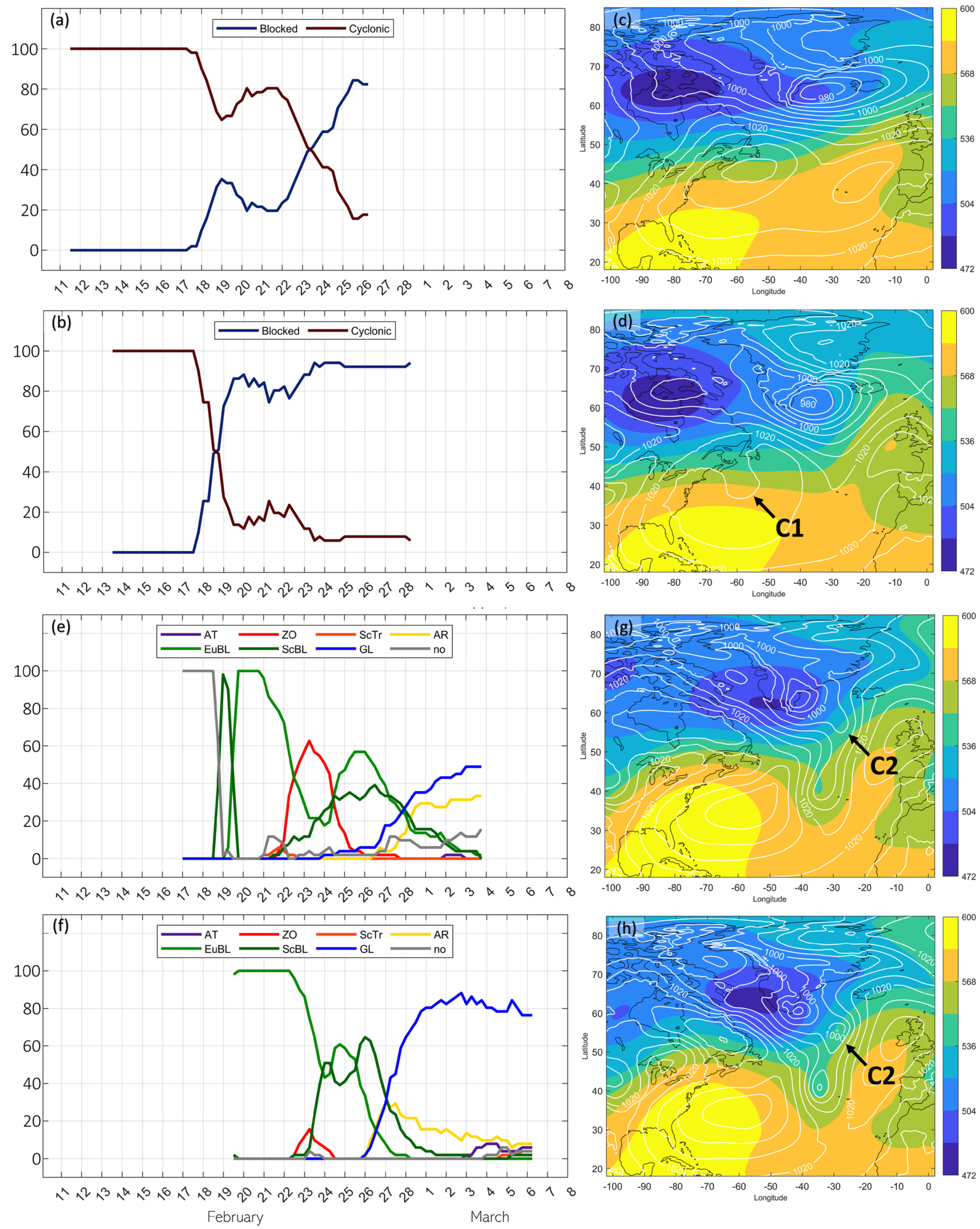
(a)
Blocked
Cyclonic
(b)
(c)
(d)
C1
(e)
(f)
AT
ZO
ScTr
AR
EuBL
ScBL
GL
no
(g)
C2
(h)
Latitude
Longitude
February
March

Figure 3.

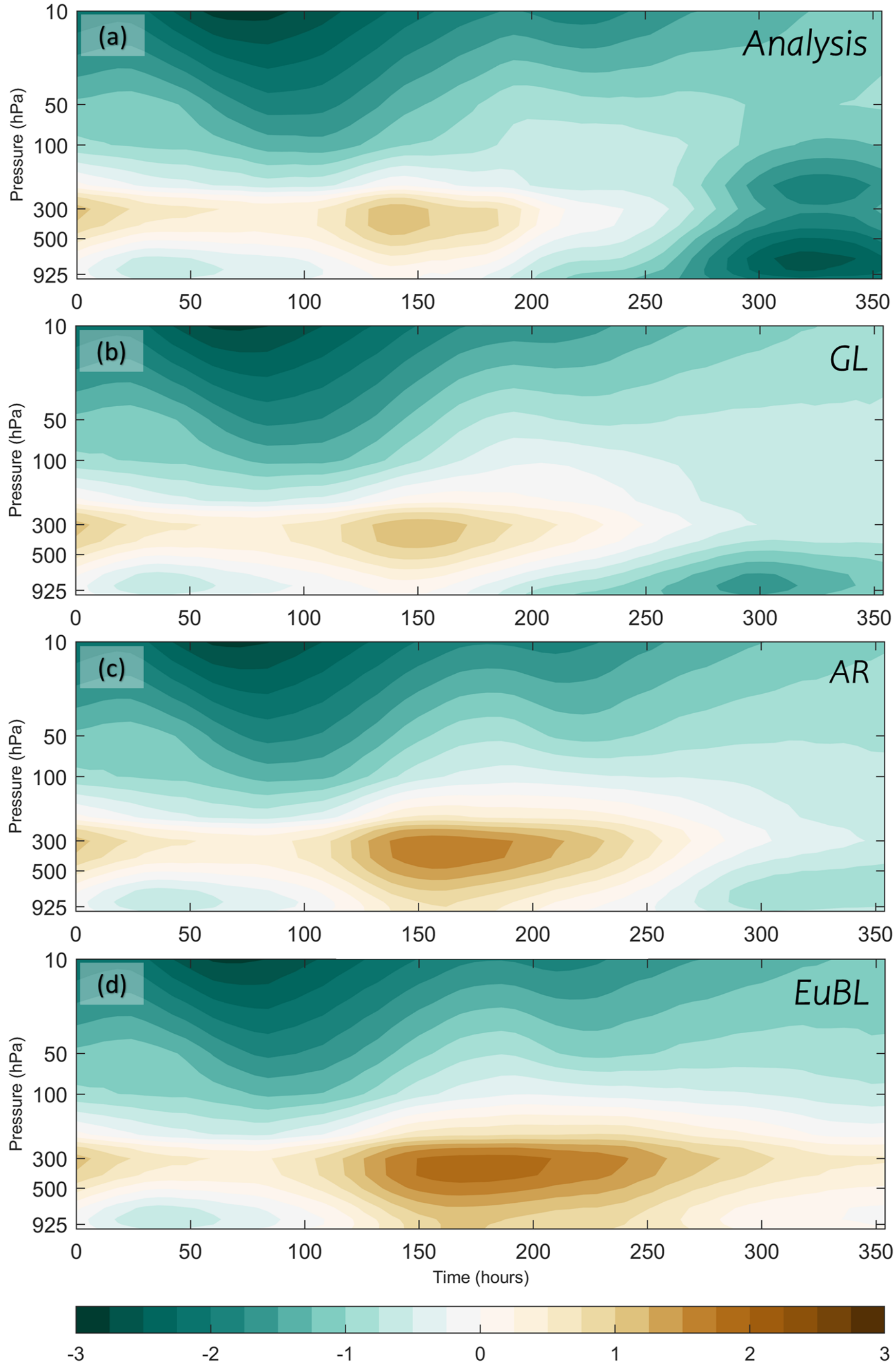

Figure 4. Time evolution of the standardized Northern Annular Mode index with lead time for, (a) analysis, (b) GL, (c) AR and, (d) EuBL composites for the 00 UTC 17 February 2018 initialization. Differences between weather regimes and the analysis are shown in Figure S10 of Supporting Information S1.

Figure 3. Probability of occurrence for blocked and cyclonic regimes for the initializations on, (a) 12 UTC 11 February 2018 and, (b) 12 UTC 13 February 2018. Ensemble MSLP (hPa; white contours) and 500-hPa geopotential height (damgp; shaded) at 00 UTC 19 February 2018 for initialization times, (c) 12 UTC 11 February 2018 and, (d) 12 UTC 13 February 2018. Probability of occurrence for all the weather regimes for the initializations on, (e) 00 UTC 17 February 2018 and, (f) 12 UTC 19 February 2018. Same as, (c) and, (d) but at 00 UTC 21 February 2018 for the initializations on (g) 00 UTC 17 February 2018 and, (h) 12 UTC 19 February 2018. Cyclogenesis 1 and 2 are indicated by C1 and C2.

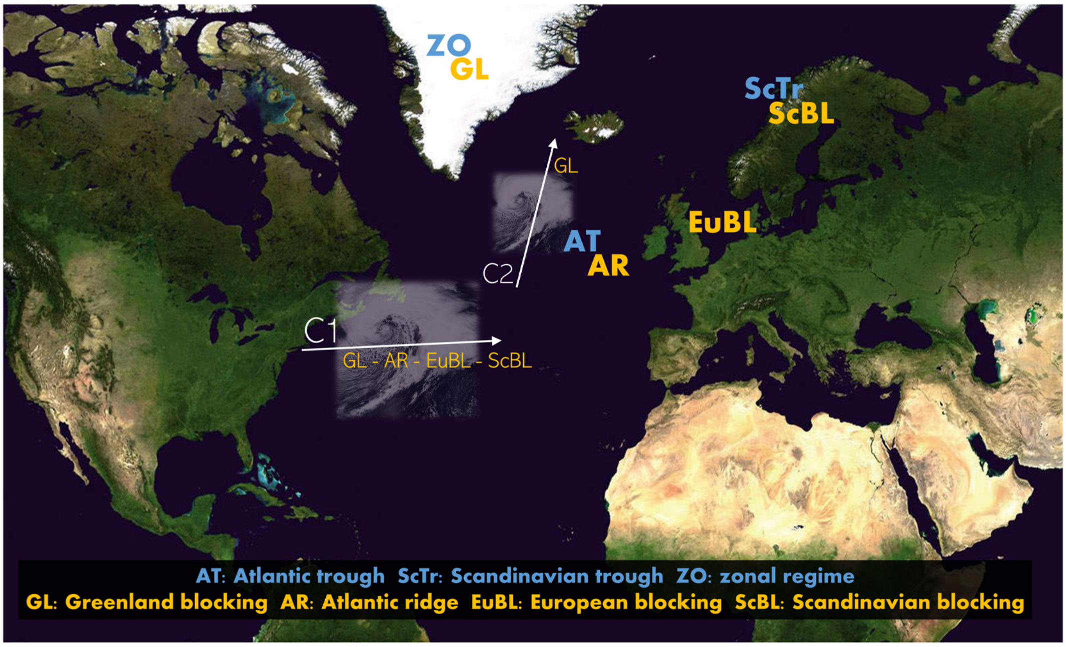

Figure 5. Schematic summary of the results: Cyclogenesis 1 (C1) developed on 19 February 2018 and provoked an increase in the occurrence probability of blocked regimes (GL+AR+EuBL+ScBL), while cyclogenesis 2 (C2), developed on 21 February 2018, mostly increased the likelihood of GL. Arrows indicate the approximate movement of the resulting cyclones. Also, weather regimes are placed in bold over the location of their centers of action, with blocked and cyclonic regimes in orange and blue, respectively.

their associated RWB, and the occurrence of GL in this event improves the representation of the observed stratosphere-troposphere coupling and thus, the SSW's surface impact.

Apart from the stratosphere, the ocean may have played a role for the cyclone errors and ensuing atmospheric circulation change (Figure S8 in Supporting Information S1). The energy taken up by the atmosphere from the ocean through latent heat fluxes (Figure S8a in Supporting Information S1) was much higher in GL than in EuBL over the central North Atlantic, just west of the Iberian Peninsula. This caused a stronger decrease in sea surface temperatures (SSTs), in a region coincident with the location of warm SST anomalies (Figure S8b in Supporting Information S1). However, sensitivity experiments do not support this connection (more information on Text S1 of Supporting Information S1). No significant differences between the experiments in the GL probability of occurrence are observed (Figure S9 in Supporting Information S1). Thus, the warm SST anomalies likely did not play a role in the establishment of GL, although they may still have influenced its persistence.

7. Conclusions and Further Research

This study focuses on predictability barriers associated with the tropospheric role in the SSW's surface impact in February 2018. The identification of the dynamics associated with these barriers can shed light on stratosphere-troposphere coupling by highlighting the tropospheric synoptic events that may have favored the coupling. We identify two important predictability barriers that occurred on 12 and 17 February 2018, between the onset of the SSW and the establishment of the GL blocking that led to the documented SSW surface impact.

Figure 5 sums up our conclusions. The identified barriers were associated with the occurrence of two extratropical cyclones in the North Atlantic. The first cyclogenesis that developed near Newfoundland plays a key role in the first increase in the number of ensemble members correctly predicting the establishment of GL, by increasing the likelihood of an atmospheric blocked state. The secondary cyclogenesis in its wake provokes the second and final increase of GL, by causing the final type of blocking to emerge. Unless these cyclogenesis events are well captured by the forecasts, the prediction of GL does not become highly prevalent.

In terms of WR analysis, these events modulate the WR probability of occurrence as follows:

1. Cyclogenesis 1 provokes an increase of likelihood for blocked WRs, associated with an anomalous ridge/high over the north-northeastern Atlantic (AR, EuBL, ScBL and GL). Before the development of this strong extratropical cyclone, the ensemble prediction system had a tendency toward the forecast of cyclonic WRs associated with an anomalous trough/low over the same region (AT, ZO, and ScTr) or no regime.
2. Cyclogenesis 2 refines the evolution toward the establishment of GL. It provokes an increase in GL probability over those WRs associated with the ridge/high by determining the exact location of the blocking. Therefore, this last event finally modulates the real response of the troposphere by facilitating the stratosphere-troposphere coupling.

This stepwise increase in predictability is consistent with that found in Kautz et al. (2020) (their Figure 10), where they focus on the forecast skill of the cold spell that affected Eurasia. Although we have here identified the tropospheric mechanism that could have favored the SSW's surface impact, we have not studied the stratosphere-troposphere coupling itself because the lower stratosphere has not been analyzed in detail. The role of lower stratospheric processes will be analyzed in subsequent work, where the potential link of these events with the stratospheric behavior will be sought.

The WR perspective employed here permits us to characterize the North Atlantic circulation beyond the commonly used bi-modal description (cyclonic vs. blocked regimes or NAO + vs. NAO-), and to handle the differences within blocked states, which are relevant for surface weather impacts (cf. Beerli & Grams, 2019 for WR projections onto NAO phases). This methodology has also allowed us to illustrate that the described WR transition during late February 2018 (Figure S1 in Supporting Information S1) was indeed one of the preferred ones described in Vautard (1990), typically associated with strong RWB (from cyclogenesis C1 and C2) south of Greenland (Benedict et al., 2004; Gómara et al., 2014; Michel & Rivière, 2011; Michel et al., 2012; Woollings et al., 2008).

While the troposphere has been shown to represent a major factor in determining the surface response to SSW events, this study clearly indicates that the tropospheric influence on the downward impact from the stratosphere may be strongly affected by the troposphere's own internal variability, and synoptic events in particular. As shown here, these synoptic events are strongly affected by predictability barriers. Thus, the predictability of the downward impact from the stratosphere will likely also strongly be affected by these same predictability barriers. While this study focuses on a particularly interesting case study, it is likely that such tropospheric predictability barriers affect the downward impact from the stratosphere and its predictability in other cases, which might explain the limited progress in obtaining improved predictability from stratospheric events over Europe (cf. Büeler et al., 2020). This finding will have to be verified for other regions that exhibit higher predictability gains after stratospheric events such as eastern Russia or the central United States (Domeisen, Butler, et al., 2020). Hence, while the stratosphere may provide a long-lived forcing that can enhance predictability in the troposphere, specifically over Europe (Sigmond et al., 2013), tropospheric predictability barriers may strongly affect the predictability of this downward impact on timescales of one to several weeks.

Acknowledgments
JJGA is funded through FJC2018-035821-I and PID2019-107125RB-I00 by the Spanish State Agency of Research, co-funded by the European Social Fund. CMG is funded by the Helmholtz Association (SPREADOUT; grant VH-NG-1243). Support from the Swiss National Science Foundation (PP00P2_170523) to DD is gratefully acknowledged. IG and BRF are supported by the EU H2020 project NextGEMS (No. 101003470) and the Spanish Ministry of Economy and Competitiveness project PRE4CAST (CGL2017-86415-R). PZ is supported by grant PID2019-109107GB-I00 and BA is supported through the JeDiS (RTI2018-096402-B-I00) project both funded by the Spanish Ministry of Science, Innovation and Universities. We would like to thank the two anonymous reviewers for their careful corrections and constructive suggestions during the review process.

Data Availability Statement

Data and code to produce results obtained in this work are publicly available at the following link: https://osf.io/xt3q9/files/

References

Ayarzagüena, B., Barriopedro, D., Garrido-Perez, J. M., Abalos, M., de la Cámara, A., García-Herrera, R., et al. (2018). Stratospheric connection to the abrupt end of the 2016/2017 Iberian drought. *Geophysical Research Letters*, *45*, 12639–12646.

Baldwin, M. P., Ayarzagüena, B., Birner, T., Butchart, N., Butler, A. H., Charlton-Perez, A. J., et al. (2021). Sudden stratospheric warmings. *Reviews of Geophysics*, *59*, e2020RG000708. https://doi.org/10.1029/2020RG000708

Baldwin, M. P., & Dunkerton, T. J. (1999). Propagation of the Arctic Oscillation from the stratosphere to the troposphere. *Journal of Geophysical Research*, *104*(D24), 30937–30946. https://doi.org/10.1029/1999jd900445

Baldwin, M. P., & Dunkerton, T. J. (2001). Stratospheric harbingers of anomalous weather regimes. *Science*, *294*(5542), 581–584. https://doi.org/10.1126/science.1063315

Beerli, R., & Grams, C. M. (2019). Stratospheric modulation of the large-scale circulation in the Atlantic–European region and its implications for surface weather events. *Quarterly Journal of the Royal Meteorological Society*, *145*, 3732–3750. https://doi.org/10.1002/qj.3653

Benedict, J. J., Sukyoung, L., & Steven, B. F. (2004). Synoptic view of the North Atlantic oscillation. *Journal of the Atmospheric Sciences*, *61*, 121–144. https://doi.org/10.1175/1520-0469(2004)061<0121:svotna>2.0.co;2

Binder, H., Boettcher, M., Grams, C. M., Joos, H., Pfahl, S., & Wernli, H. (2017). Exceptional air mass transport and dynamical drivers of an extreme wintertime Arctic warm event. *Geophysical Research Letters*, *44*, 12028–12036. https://doi.org/10.1002/2017GL075841

Büeler, D., Beerli, R., Wernli, H., & Grams, C. M. (2020). Stratospheric influence on ECMWF sub-seasonal forecast skill for energy-industry-relevant surface weather in European countries. *Quarterly Journal of the Royal Meteorological Society*, *146*, 3675–3694, https://doi.org/10.1002/qj.3866

Chan, C. J., & Plumb, R. A. (2009). The response to stratospheric forcing and its dependence on the state of the troposphere. *Journal of the Atmospheric Sciences*, *66*(7), 2107–2115. https://doi.org/10.1175/2009JAS2937.1

Colucci, S. J. (1985). Explosive cyclogenesis and large-scale circulation changes: Implications for atmospheric blocking. *Journal of the Atmospheric Sciences*, *42*, 2701–2717. https://doi.org/10.1175/1520-0469(1985)042<2701:ecalsc>2.0.co;2

Dee, D. P., Uppala, S. M., Simmons, A. J., Berrisford, P., Poli, P., Kobayashi, S., et al. (2011). The ERA-Interim reanalysis: Configuration and performance of the data assimilation system. *Quarterly Journal of the Royal Meteorological Society*, *137*, 553–597. https://doi.org/10.1002/qj.82

Domeisen, D. I., Butler, A. H., Charlton-Perez, A. J., Ayarzagüena, B., Baldwin, M. P., Dunn-Sigouin, E., et al. (2020). The role of the stratosphere in subseasonal to seasonal prediction: 2. Predictability arising from stratosphere-troposphere coupling. *Journal of Geophysical Research: Atmospheres*, *125*, e2019JD030923. https://doi.org/10.1029/2019JD030923

Domeisen, D. I. V., & Butler, A. H. (2020). Stratospheric drivers of extreme events at the Earth's surface. *Communications Earth & Environment*, *1*, 59. https://doi.org/10.1038/s43247-020-00060-z

Domeisen, D. I. V., Grams, C. M., & Papritz, L. (2020). The role of North Atlantic–European weather regimes in the surface impact of sudden stratospheric warming events. *Weather and Climate Dynamics*, *1*(2), 373–388. https://doi.org/10.5194/wcd-1-373-2020

Domeisen, D. I. V., Sun, L., & Chen, G. (2013). The role of synoptic eddies in the tropospheric response to stratospheric variability. *Geophysical Research Letters*, *40*, 1–4937. https://doi.org/10.1002/grl.50943

ECMWF. (2020). IFS documentation for model cycle 41r1. ECMWF. Technical Report Accessed 19 June 2021. Retrieved from https://confluence.ecmwf.int/display/FCST/Detailed+information+of+implementation+of+IFS+cycle+41r2

Garfinkel, C. I., Waugh, D. W., & Gerber, E. P. (2013). The effect of tropospheric jet latitude on coupling between the stratospheric polar vortex and the troposphere. *Journal of Climate*, *26*(6), 2077–2095. https://doi.org/10.1175/JCLI-D-12-00301.1

Gómara, I., Pinto, J. G., Woollings, T., Masato, G., Zurita-Gotor, P., & Rodríguez-Fonseca, B. (2014). Rossby wave-breaking analysis of explosive cyclones in the Euro-Atlantic sector. *Quarterly Journal of the Royal Meteorological Society*, *140*, 738–753. https://doi.org/10.1002/qj.2190

Grams, C. M., Magnusson, L., & Madonna, E. (2018). An atmospheric dynamics perspective on the amplification and propagation of forecast error in numerical weather prediction models: A case study. *Quarterly Journal of the Royal Meteorological Society*, *144*, 2577–2591. https://doi.org/10.1002/qj.3353

Kautz, L.-A., Polichtchouk, I., Birner, T., Garny, H., & Pinto, J. G. (2020). Enhanced extended-range predictability of the 2018 late-winter Eurasian cold spell due to the stratosphere. *Quarterly Journal of the Royal Meteorological Society*, *146*, 1040–1055. https://doi.org/10.1002/qj.3724

Maddison, J. W., Gray, S. L., Martínez-Alvarado, O., & Williams, K. D. (2019). Upstream cyclone influence on the predictability of block onsets over the Euro-Atlantic Region. *Monthly Weather Review*, *147*(4), 1277–1296. https://doi.org/10.1175/mwr-d-18-0226.1

Meehl, G. A., Richter, J. H., Teng, H., Capotondi, A., Cobb, K., Doblas-Reyes, F., et al. (2021). Initialized Earth System prediction from subseasonal to decadal timescales. *Nature Reviews Earth & Environment*, 1–18. https://doi.org/10.1038/s43017-021-00155-x

Michel, C., & Rivière, G. (2011). The link between rossby wave breakings and weather regime transitions. *Journal of the Atmospheric Sciences*, *68*, 1730–1748. https://doi.org/10.1175/2011JAS3635.1

Michel, C., Rivière, G., Terray, L., & Joly, B. (2012). The dynamical link between surface cyclones, upper-tropospheric Rossby wave breaking and the life cycle of the Scandinavian blocking. *Geophysical Research Letters*, *39*, L10806. https://doi.org/10.1029/2012GL051682

Pfahl, S., Schwierz, C., Croci-Maspoli, M., Grams, C. M., & Wernli, H. (2015). Importance of latent heat release in ascending air streams for atmospheric blocking. *Nature Geoscience*, *8*, 610–614. https://doi.org/10.1038/ngeo2487

Rao, J., Garfinkel, C. I., & White, I. P. (2020). Predicting the downward and surface influence of the February 2018 and January 2019 sudden stratospheric warming events in subseasonal to seasonal (S2S) models. *Journal of Geophysical Research: Atmospheres*, *125*, e2019JD031919. https://doi.org/10.1029/2019JD031919

Rupp, P., & Birner, T. (2021). Tropospheric eddy feedback to different stratospheric conditions in idealised baroclinic life cycles. *Weather and Climate Dynamics*, *2*, 111–128. https://doi.org/10.5194/wcd-2-111-2021

Sánchez, C., Methven, J., Gray, S., & Cullen, M. (2020). Linking rapid forecast error growth to diabatic processes. *Quarterly Journal of the Royal Meteorological Society*, *146*, 3548–3569. https://doi.org/10.1002/qj.3861

Sigmond, M., Scinocca, J. F., Kharin, V. V., & Shepherd, T. G. (2013). Enhanced seasonal forecast skill following stratospheric sudden warmings. *Nature Geoscience*, *6*(2), 98–102. https://doi.org/10.1038/ngeo1698

Steinfeld, D., Boettcher, M., Forbes, R., & Pfahl, S. (2020). The sensitivity of atmospheric blocking to upstream latent heating – Numerical experiments. *Weather and Climate Dynamics*, *1*, 405–426. https://doi.org/10.5194/wcd-1-405-2020

Vautard, R. (1990). Multiple weather regimes over the North Atlantic: Analysis of precursors and successors. *Monthly Weather Review*, *118*(10), 2056–2081. https://doi.org/10.1175/1520-0493(1990)118<2056:mwrotn>2.0.co;2

Wilks, D. S. (2006). *Statistical Methods in the Atmospheric Sciences* (Vol. 14). Meteorological Applications.

Woollings, T., Hoskins, B., Blackburn, M., & Berrisford, P. (2008). A new Rossby wave-breaking interpretation of the North Atlantic Oscillation. *Journal of the Atmospheric Sciences*, *65*(2), 609–626. https://doi.org/10.1175/2007jas2347.1